

Structures of Pathogenic Fungal FKBP12s Reveal Possible Self-Catalysis Function

Nam K. Tonthat,^a Praveen Rao Juvvadi,^b Hengshan Zhang,^a Soo Chan Lee,^c Ron Venters,^a Leonard Spicer,^{a,d} William J. Steinbach,^{b,c} Joseph Heitman,^c Maria A. Schumacher^a

Department of Biochemistry, Duke University School of Medicine, Durham, North Carolina, USA^a; Department of Pediatrics, Division of Pediatric Infectious Diseases, Duke University School of Medicine, Durham, North Carolina, USA^b; Department of Molecular Genetics and Microbiology, Duke University School of Medicine, Durham, North Carolina, USA^c; Department of Radiology, Duke University School of Medicine, Durham, North Carolina, USA^d

ABSTRACT Invasive fungal infections remain difficult to treat and require novel targeting strategies. The 12-kDa FK506-binding protein (FKBP12) is a ubiquitously expressed peptidyl-prolyl isomerase with considerable homology between fungal pathogens and is thus a prime candidate for future targeting efforts to generate a panfungal strategy. Despite decades of research on FKBP, their substrates and mechanisms of action remain unclear. Here we describe structural, biochemical, and *in vivo* analyses of FKBP12s from the pathogenic fungi *Candida albicans*, *Candida glabrata*, and *Aspergillus fumigatus*. Strikingly, multiple apo *A. fumigatus* and *C. albicans* FKBP12 crystal structures revealed a symmetric, intermolecular interaction involving the deep insertion of an active-site loop proline into the active-site pocket of an adjacent subunit. Such interactions have not been observed in previous FKBP structures. This finding indicates the possibility that this is a self-substrate interaction unique to the *A. fumigatus* and *C. albicans* fungal proteins that contain this central proline. Structures obtained with the proline in the *cis* and *trans* states provide more data in support of self-catalysis. Moreover, cysteine cross-linking experiments captured the interacting dimer, supporting the idea that it forms in solution. Finally, genetic studies exploring the impact of mutations altering the central proline and an adjacent residue provide evidence that any dimeric state formed *in vivo*, where FKBP12 concentrations are low, is transient. Taken together, these findings suggest a unique mechanism of self-substrate regulation by fungal FKBP12s, lending further novel understanding of this protein for future drug-targeting efforts.

IMPORTANCE FKBP12 is a *cis-trans* peptidyl-prolyl isomerase that plays key roles in cellular protein homeostasis. FKBP12s also bind the immunosuppressive drug FK506 to inhibit the phosphatase calcineurin (CaN). CaN is required for virulence of *A. fumigatus*, *C. albicans*, *C. glabrata*, and other deadly fungal pathogens, marking FKBP12 and CaN as potential broad-spectrum drug targets. Here we describe structures of fungal FKBP12s. Multiple apo *A. fumigatus* and *C. albicans* FKBP12 structures reveal the insertion of a proline, conspicuously conserved in these proteins, into the active sites of adjacent molecules. This suggests that these proteins might serve as their own substrates. Cysteine disulfide trapping experiments provide support for this self-interaction and hence possible intermolecular catalysis by these enzymes.

Received 17 March 2016 Accepted 28 March 2016 Published 26 April 2016

Citation Tonthat NK, Juvvadi PR, Zhang H, Lee SC, Venters R, Spicer L, Steinbach WJ, Heitman J, Schumacher MA. 2016. Structures of pathogenic fungal FKBP12s reveal possible self-catalysis function. mBio 7(2):e00492-16. doi:10.1128/mBio.00492-16.

Editor Patricia J. Johnson, UCLA

Copyright © 2016 Tonthat et al. This is an open-access article distributed under the terms of the [Creative Commons Attribution 4.0 International license](https://creativecommons.org/licenses/by/4.0/).

Address correspondence to Maria A. Schumacher, maria.schumacher@duke.edu.

This article is a direct contribution from a Fellow of the American Academy of Microbiology. External solicited reviewers: Ping Wang, Children's Hospital; Jun Liu, Johns Hopkins University School of Medicine.

The 12-kDa FK506-binding protein (FKBP12) is a peptidyl-prolyl isomerase (PPIase) that is ubiquitously expressed in prokaryotic and eukaryotic cells and is a member of the FKBP PPIase superfamily (1–23). In addition to FKBP, there are two additional classes of PPIases, the cyclophilins and the parvulins (10). PPIase proteins all catalyze the *cis/trans* isomerization of peptide bonds N terminal to proline residues in polypeptide chains. It is estimated that 5 to 7% of the proteins in eukaryotes that possess a peptidyl-prolyl bond acquire a *cis* conformation during folding. There is a large energy barrier of 14 to 24 kcal/mol between the *cis* and *trans* states, and hence, *cis/trans* isomerization is intrinsically slow and often represents the rate-limiting step in protein folding events (1–3). Therefore, PPIases, which catalyze this conformational change, play a central role in protein homeostasis in all cells (1–23).

In addition to its role as a PPIase, FKBP12 is a member of the immunophilin family and is the target of the immunosuppressive drugs FK506 and rapamycin (24–27). The FKBP12-FK506 complex binds the phosphatase calcineurin (CaN) and prevents it from dephosphorylating its downstream targets. CaN dephosphorylates the cytoplasmic component of the nuclear factor of activated T cells (NF-AT) transcription factor, which is necessary for interleukin-2 transcription and T-cell activation (28–32). As a result, inhibition of this key CaN function by FKBP12-FK506 leads to immunosuppression. CaN is also essential for the pathogenesis of some of the most deadly human fungal pathogens, including *Candida albicans*, *Candida glabrata*, and *Aspergillus fumigatus* (31). The fungal FKBP12 sequences are only 40–50% identical to their human counterpart, compared to the nearly

TABLE 1 Data collection and refinement statistics for *C. albicans* FKBP12 structures

Parameter	<i>C. albicans</i> FKBP12 apo form:			<i>C. albicans</i> FKBP12(P104G)-FK506	Apo <i>C. albicans</i> FKBP12(P104G)
	1	2	3		
Space group	C2	P2 ₁ 2 ₁ 2	P1	C2	P2 ₁
Unit cell dimensions					
<i>a</i> , <i>b</i> , <i>c</i> (Å)	99.5, 43.0, 70.7	35.8, 80.7, 94.9	35.9, 38.6, 50.4	115.4, 84.2, 116.7	51.2, 44.0, 56.99
$\alpha = \beta = \gamma$ (°)	90.0, 128.2, 90.0	90.0, 90.0, 90.0	78.6, 69.7, 79.3	90.0, 109.8, 90.0	90.0, 115.0, 90.0
Resolution (Å)	26.0-2.4	40.9-2.3	63.8-1.99	26.1-2.9	45.3-2.0
<i>R</i> _{merge} (%)	10.1 (19.7) ^a	6.4 (55.9)	9.1 (31.2)	12.4 (38.7)	4.5 (17.3)
<i>I</i> / σ - <i>I</i>	13.2 (6.3)	23.6 (2.0)	5.8 (2.0)	10.7 (2.1)	20.8 (2.2)
Completeness (%)	98.2 (93.8)	98.8 (92.3)	85.2 (85.2)	84.3 (37.6)	99.0 (89.8)
Redundancy	3.3 (2.4)	3.0 (2.2)	1.6 (1.6)	2.8 (1.4)	3.3 (2.9)
Refinement					
Resolution range (Å)	25.96–2.4	40.9–2.3	63.8–1.99	26.1–2.9	45.3–2.0
<i>R</i> _{work} / <i>R</i> _{free} (%)	17.7/22.2	17.9/22.8	22.5/25.4	24.4/28.5	18.0/19.5
No. of atoms					
Protein	1,733	1,808	2,056	6,769	3,788
Water	129	67	166	64	161
RMSD					
Bond length (Å)	0.004	0.008	0.002	0.008	0.003
Bond angle (°)	0.86	1.42	1.29	1.59	0.88

^a Values in parentheses are for the highest-resolution shell.

identical interacting regions in the catalytic and regulatory domains of CaN proteins. Hence, fungal FKBP12s have emerged as potential targets for the development of broadly acting antifungal agents (21). The development of novel antifungal agents that specifically target the FKBP12 component in this pathway would be significantly aided by the structural elucidation of these proteins.

While there are currently no structures available for the fungal pathogen FKBP12s, multiple structures of FKBP12 and higher-molecular-weight FKBP12s from humans and other organisms (including the model yeast *Saccharomyces cerevisiae*) have been determined in both their apo states and in complex with FK506 and rapamycin (27, 33, 34). These structures reveal that the FKBP12s share the same overall fold that includes a five- to six-stranded β -sheet that wraps around an α -helix. Three extended loops, which have been called the 40s loop (between β 2 and β 3), the 50s loop (between β 3' and α 1), and the 80s loop (between β 4 and β 5), surround a deep active-site pocket that binds both FK506 and rapamycin (18, 19). Despite the numerous structural, biochemical, and *in vivo* studies of FKBP12s that have been carried out, their substrate specificities and catalytic mechanisms are still unclear. Indeed, there are no structures available for an FKBP12-substrate complex. The only structure that gives some insight into this enzyme-substrate interaction is the structure of the FKBP domain from *Plasmodium vivax* FKBP35 (PvFKBP35) in complex with the unnatural tetrapeptide substrate succinyl-Ala-Leu-Pro-Phe-*p*-nitroanilide (35). However, the physiological relevance of this structure is unclear, as data showed that PvFKBP35 is a monomer and in the crystal structure the substrate peptide is bound between two subunits of a crystallographic dimer.

To gain insight into the structure and function of the FKBP12s of *C. albicans*, *C. glabrata*, and *A. fumigatus*, we performed structural, biochemical, and genetic studies. Strikingly, the *C. albicans* and *A. fumigatus* FKBP12 apo structures all revealed the deep insertion of a proline located in the 80s loop into the ligand-binding pocket of a neighboring FKBP12 subunit. This interaction was not observed in the *C. glabrata* structure, which does not have the corresponding proline residue. Comparison of the apo struc-

tures with FKBP12-FK506 complexes reveals that this “self-substrate” overlaps the binding site of FK506. As FK506 is a transition state analog, these data suggest the possibility that these fungal FKBP12s might function as their own substrates. To test this hypothesis, we generated a single-cysteine mutant that was able to trap the self-interacting dimer, showing that it forms in solution. We also performed genetic studies to probe the effects of mutations in the 80s loop of *A. fumigatus* FKBP12. The combined studies support the possibility that the *A. fumigatus* and *C. albicans* FKBP12s may function as their own substrates, lending unique insight into this conserved and targetable fungal protein.

RESULTS

Structures of the apo *A. fumigatus* and *C. albicans* FKBP12s.

The *C. albicans* and *A. fumigatus* FKBP12s represent potential drug targets in treating invasive fungal infections. To gain insight into the structures and functions of these proteins, we determined their crystal structures. Three different crystal forms of the apo *C. albicans* FKBP12, to resolutions of 1.99, 2.3, and 2.4 Å, were obtained (Table 1). The FKBP12 subunit structures of the three crystal forms are essentially identical (root mean square deviations [RMSDs] of ~0.2 to 0.4 Å for superimpositions of corresponding C- α atoms) (Fig. 1A and B). Structural homology searches with DALI revealed that the *C. albicans* apo FKBP12 structures show significant structural homology to all FKBP12s, with the strongest similarity to the human protein (Protein Data Bank [PDB] code 1d7h); superimposition of corresponding C- α atoms of the *C. albicans* and human FKBP12 structures resulted in an RMSD of 1.02 Å (Fig. 1C). Like other FKBP12 structures, the *C. albicans* protein harbors the typical core FKBP12 structure, which consists of a five-stranded β -sheet wrapped about the central helix. In addition, *C. albicans* FKBP12 has an insert of 12 residues between α 1 and β 4 (Fig. 1A and C). Despite the extra residues in the insert region of the *C. albicans* structure, it contains the same pocket as other FKBP12s, which is framed by the 40s, 50s, and 80s loops (Fig. 1C).

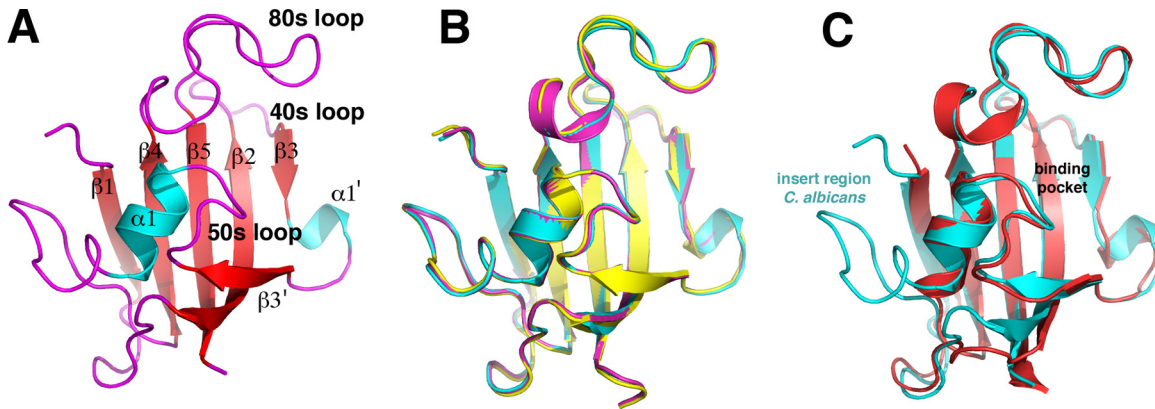


FIG 1 Crystal structures of *C. albicans* apo FKBP12. (A) Overall structure of the *C. albicans* FKBP12 apo form with the β -strand colored red, helices colored cyan, loops colored magenta, and secondary structural elements labeled. (B) Overlaid structures of the three crystal forms of *C. albicans* apo FKBP12 showing their overall identity. (C) Overlaid *C. albicans* (cyan) and human (red) FKBP12 structures. Labeled is the insert region that is not present in the human protein.

***C. albicans* apo FKBP12 structures reveal intermolecular contacts between active sites.** While the *C. albicans* apo FKBP12 structure is very similar to previously determined FKBP12 structures, an unexpected finding that emerged from analysis of the crystal packing was that despite being obtained under very different crystallization conditions with distinct crystal lattices, all three

C. albicans apo FKBP12 structures displayed the same intermolecular interactions between subunits (Fig. 2A). What is notable about this interaction is that the 80s loop of one subunit docks into the active site of the adjacent subunit and vice versa, suggesting that the loop may act as a substrate. Indeed, Pro104, which is located at the tip of the loop, is inserted most deeply into the

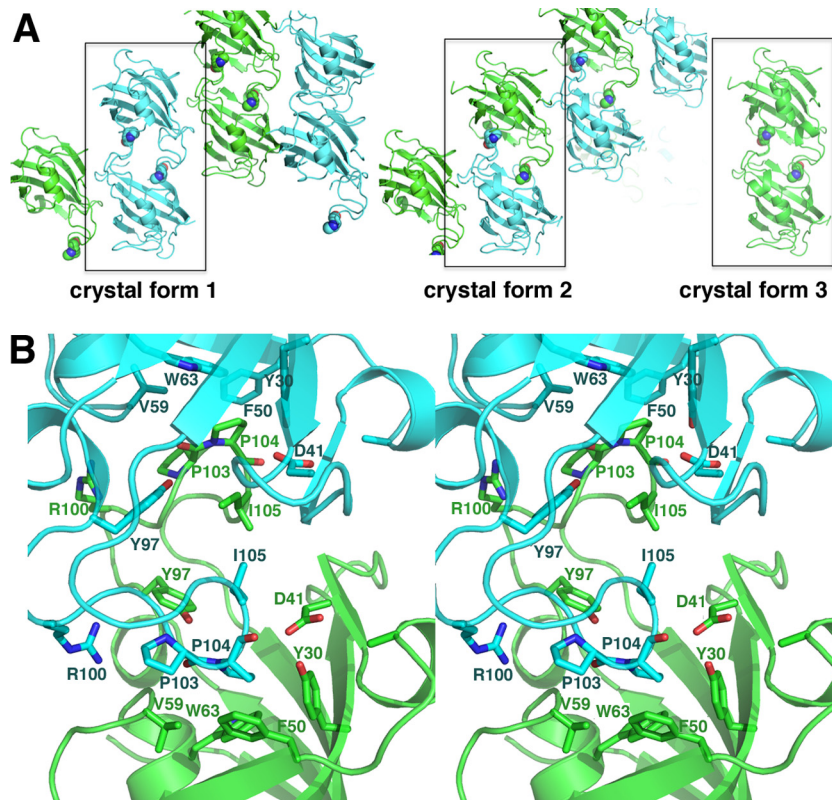


FIG 2 Intermolecular active-site cross contacts revealed in *C. albicans* apo structures. (A) Packing of the three crystal forms of *C. albicans* apo FKBP12. In all cases, an intermolecular active-site cross contact is formed in which the 80s loop is inserted into the active site of an adjacent molecule. The interaction is symmetric, and hence, each dimer has two “substrate” interactions. Pro104, which is located at the tip of the 80s loop and shown as a CPK model, is the most deeply inserted side chain, and it contacts key residues shown to be important for FKBP12 PPIase activity. (B) Stereo view of the two-fold related 80s loop active-site interactions in the *C. albicans* apo FKBP12 structures. Notably, a previous study (36) showed that residues Asp41, Val59, and Tyr97 are critical for FKBP12 PPIase activity. In the structures, these residues directly contact or form part of the pocket for binding of the Pro104 side chain. Notably, the Asp41 side chain makes hydrogen bonds with the Pro104 carbonyl oxygen in each pocket.

pocket and is surrounded by residues that have been implicated, via mutagenesis, to be involved in FKBP PPIase activity (36, 37). Three residues, in particular, were implicated as important for FKBP12 catalysis and correspond to Val59, Asp41, and Tyr97 in the *C. albicans* protein (Fig. 2B). These residues all make direct contacts with Pro104, which rests within an aromatic cleft formed by Tyr30, Phe50, and Trp63 (Fig. 2B). Notably, the interface in the *C. albicans* FKBP12-FKBP12 interaction is minimal (burying 592 Å² from solvent), which suggests that, like known substrate-enzyme complexes, the proteins form a weak interaction; typical dimer interfaces bury >2,000 Å² of surface from solvent. Although most of the contacts that hold the loop in position in the active site are with the central Pro104, additional hydrophobic contacts with Ile102, Pro103, and Ile105 are provided, while Arg100 makes hydrogen bonds with the carbonyl oxygens at the edge of the pocket.

Studies have indicated that the immunosuppressant FK506 functions as a transition state mimic when bound to FKBP12 (19). Comparison of the *C. albicans* FKBP12 apo structure with FKBP12-FK506 structures reveals that the 80s loop binds in the same pocket as FK506. However, to confirm that this is indeed the catalytic pocket in the *C. albicans* protein, we next sought to determine the *C. albicans* FKBP12-FK506 structure. Interestingly, initial attempts to obtain crystals of the protein-FK506 complex failed, as the intermolecular interaction appeared to be strongly favored, leading to the production of the same apo crystal forms. Thus, we generated a P104G mutation in *C. albicans* FKBP12 and crystallized and obtained the apo FKBP12(P104G) structure to 2.0 Å (Table 1). Strikingly, this structure did not harbor the self-catalysis-like interaction (see Fig. S1 in the supplemental material). We next used the FKBP12(P104G) protein to obtain the structure bound to FK506 (Table 1). The structure revealed that, similar to other FKBP12-FK506 complexes, the immunosuppressant binds in the active-site pocket, surrounded by the 40s, 50s, and 80s loops. Comparison of this structure with the apo *C. albicans* structures with bound self-substrates revealed that the 80s loop that is inserted into the active site of the adjacent subunit binds in precisely the same location as the FK506 substrate/transition state homolog (Fig. 3).

A. *fumigatus* FKBP12 structures: self-catalysis captured?

Our data thus far revealed that *C. albicans* FKBP12 contains a proline residue at the tip of its 80s loop, Pro104, that, in the apo form, is inserted into the active site of a neighboring subunit. Sequence alignments revealed that *A. fumigatus* FKBP12 contains the same proline residue in its 80s loop that makes intermolecular interactions in the *C. albicans* protein (Table 2; Fig. 4A). Thus, to deduce if *A. fumigatus* FKBP12 might form a similar self-substrate-like interaction, we crystallized and determined the structure of the apo form of the protein. Remarkably, we observed the same insertion of the 80s loop of each subunit into the active site of the other subunit (Fig. 4B). As for *C. albicans* FKBP12, we also had difficulty obtaining the structure of the *A. fumigatus* wild-type (WT) protein in complex with FK506. Thus, we generated the analogous mutation, P90G, and used that protein to obtain the FKBP12(P90G)-FK506 structure. As expected the FK506 molecule is bound in the same active-site pocket of *A. fumigatus* FKBP12 as in other FKBP12-FK506 complex structures (Fig. 4C). Interestingly, unlike the *C. albicans* apo FKBP12 structures, which were all captured with Pro104 in the *cis* conformation, in the *A. fumigatus* structure, Pro90 in one subunit was bound in the *cis* con-

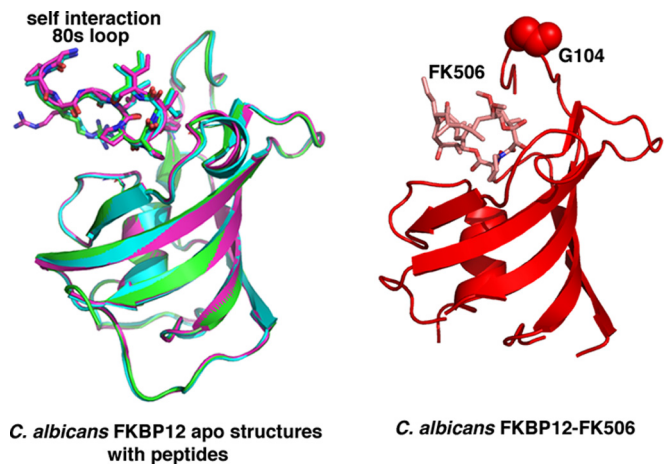


FIG 3 The 80s loop of the *C. albicans* FKBP12 apo structures binds in the same pocket as the transition state mimic FK506. On the left are overlays of the three *C. albicans* apo FKBP12 structures with the 80s loop “substrate” included. On the right is the structure of *C. albicans* FKBP12-FK506. The 80s loops from the apo structures are inserted in the same way and in the same pocket as the transition state mimic FK506 (right).

formation and Pro90 in the other was bound in the *trans* state, thus potentially providing a snapshot of self-catalysis (Fig. 4B).

***C. glabrata* FKBP12 structures.** Sequence alignments of FKBP12s from various fungal pathogens revealed that only the *A. fumigatus* and *C. albicans* proteins contain a central proline in the 80s loop. Another clinically important and often antifungal-resistant *Candida* species, *C. glabrata*, contains a glycine at this location, suggesting that this protein would not form the intermolecular interaction. To test this prediction, we determined the structures of *C. glabrata* FKBP12 in its apo and FK506-bound states (Table 3). Examination of the packing revealed a close contact between the 80s loop of one subunit and an adjacent molecule in the apo crystals. However, here the 80s loop is not inserted into the active site of the neighboring molecule. Hence, as predicted, the *C. glabrata* FKBP12 structure shows no evidence of an intermolecular self-catalysis-like binding event (see Fig. S2 in the supplemental material). However, to ensure that it utilizes the same active site, we obtained the structure in the presence of FK506 to 1.3 Å. As this structure clearly shows, FK506 binds to the active-site pocket by using a binding mode identical to that used by *C. albicans*, *A. fumigatus*, and other FKBP12s, including human FKBP12 (Fig. 4C).

Disulfide cross-linking captures the FKBP12 intermolecular interaction. While every structure of the WT apo *A. fumigatus* and *C. albicans* FKBP12s revealed the same interproline interaction, even under very diverse crystallization conditions, it remained possible that these were all crystallization artifacts. Thus, to assess if this interaction occurs in solution, we made a single cysteine mutation, V91C, in the *A. fumigatus* protein to try to capture a disulfide cross-linked complex. This residue was chosen for mutation because the structure revealed that the V91 and V91' (where the prime indicates the other subunit of the dimer) side chains are within <4.0 Å of each other and that when they are mutated to cysteines *in silico* they could form a disulfide bond in the intermolecular dimer. The *A. fumigatus* FKBP12(V91C) mutant was expressed in two *Escherichia coli* cell lines, C41(DE3) and SHuffle cells (see Materials and Methods). SHuffle cells constitu-

TABLE 2 Data collection and refinement statistics for *A. fumigatus* FKBP12 structures

Parameter	Apo <i>A. fumigatus</i> FKBP12	<i>A. fumigatus</i> FKBP12(P90G)-FK506	<i>A. fumigatus</i> FKBP12(V91C) dimer
Space group	P2 ₁ 2 ₁	P2 ₁ 2 ₁	P6 ₃
Cell dimensions			
<i>a</i> , <i>b</i> , <i>c</i> (Å)	44.8, 50.8, 103.0	37.0, 51.1 55.6	136.8, 136.8, 33.0
α , β , γ (°)	90.0, 90.0, 90.0	90.0, 90.0, 90.0	90.0, 90.0, 120.0
Resolution (Å)	45.6–2.3	37.6–2.0	44.8–3.2
<i>R</i> _{merge} (%)	6.9 (36.6) ^a	5.7 (19.5)	10.4 (56.9)
<i>I</i> / σ <i>I</i>	18.5 (3.1)	19.7 (1.8)	8.9 (1.8)
Completeness (%)	98.7 (91.2)	90.3 (99.1)	99.9 (98.6)
Redundancy	4.2 (2.6)	5.2 (5.2)	4.6 (3.6)
Refinement			
Resolution (Å)	45.6–2.3	37.6–2.0	44.8–3.2
<i>R</i> _{work} / <i>R</i> _{free} (%)	20.5/25.8	16.6/22.5	20.1/26.9
No. of atoms			
Protein	1,706	862	1,692
Water	115	147	0
RMSD			
Bond length (Å)	0.002	0.007	0.011
Bond angle (°)	0.72	1.22	2.09

^a Values in parentheses are for the highest-resolution shell.

tively express a chromosomal copy of the disulfide bond isomerase DsbC, which promotes disulfide bond formation in the cytoplasm. When the proteins were purified from both strains in the absence of a reducing agent and subjected to nonreducing SDS-PAGE, the samples revealed the presence of two species, which were consistent with FKBP12 monomers and dimers (Fig. 5A). While the protein was not as well expressed in SHuffle cells, the samples purified from these cells ran primarily as dimers. When a reducing agent (β -mercaptoethanol) was added, the proteins ran as monomers (Fig. 5A). However, to ensure that the dimeric species in the gel was not an impurity that was sensitive to the reducing agent, we performed mass spectrometry of the dimer and monomer bands. The results confirmed that both species contained the *A. fumigatus* FKBP12(V91C) protein (data not shown).

We next separated the V91C dimer from the monomer via size exclusion chromatography and crystallized and solved the structure of the dimer to 3.2 Å resolution. The structure revealed a disulfide cross-linked dimer. Interestingly, although revealing the same general dimer that we observed in the *A. fumigatus* and *C. albicans* apo FKBP12 structures, in the FKBP12(V91C) structure (Fig. 5B), Pro90 is slightly shifted from the active site and adopts a twisted conformation (Fig. 5C and D), suggesting that the structure may have captured an intermediate state of catalysis. In fact, the conformation of the Pro90 residues in the structure is closer to the *trans* than the *cis* state and overlays of the *trans* state of the protein to form an all-*trans* dimer revealed a clash. This finding suggests the intriguing possibility that part of the mechanism of prolyl isomerization by FKBP12 is dictated by the conformation of the substrate during catalysis. Indeed, the *cis* and *trans* states lead to structural changes in the loops and one state may be more favorable for binding of the active-site pocket than the other, thus determining the progress of the reaction.

Examination of the *A. fumigatus* FKBP12 interaction via Y2H analysis. To next assess if we could detect the *A. fumigatus* FKBP12 self-interaction *in vivo*, we employed the yeast two-hybrid (Y2H) system. The pGADT7 and pGBKT7 vectors, which express the GAL4 activation domain (AD) and the DNA-binding domain (BD), respectively, were employed for these studies (see Materials and Methods; see Table S1 in the supplemental mate-

rial). We utilized a specialized host strain (SMY4-1) derived from the Y2H host strain Y190 and rendered FK506 and rapamycin resistant by *fpr1::ADE2* and *TOR1-3* mutations that allow testing of the impact of these FKBP12 ligands on any interactions detected (38). *A. fumigatus* WT FKBP12, FKBP12(P90G), and FKBP12(V91C) were tested. The N or C termini of the FKBP12s were fused with the AD (e.g., Fkba-AD or AD-Fkba), and the N termini of the FKBP12s were fused with the BD (e.g., BD-Fkba) (see Table S1). Interactions were assessed in the presence or absence of FK506 (1 μ g/ml) or rapamycin (1 μ g/ml) (see Materials and Methods) (38). These experiments revealed no strong self-interactions between the FKBP12s, suggesting that the proteins did not form stable dimers in the environment of the *S. cerevisiae* nucleus (Table 4; see Fig. S3 in the supplemental material). However, this was not necessarily surprising, since we did not expect strong interactions, given the low *in vivo* concentration of FKBP12 in the cell compared to that used for crystallization. Indeed, enzyme-substrate interactions cannot be tight, as that would prevent product turnover.

Interestingly, we did observe that there is potential variation in the interaction affinity between FKBP12 and its variants during control interactions with the FKBP12-rapamycin complex-binding (FRB) domain of the TOR protein. Specifically, when the N terminus of FKBP12 or FKBP12(V91C) was linked with the AD [AD-Fkba or AD-Fkba(V91C)], it did not interact with the FRB domain in the presence of rapamycin, in contrast to other fungal FKBP12s, which revealed a strong interaction with the FRB domain under these conditions (39, 40). On the other hand, *A. fumigatus* AD-FKBP12(P90G) did reveal an interaction with the FRB domain in the presence of rapamycin. These data suggest that the properties of *A. fumigatus* FKBP12 may be altered by changing the amino acid at the 90th residue from proline to glycine.

We do not think that the failure to observe AD-Fkba or AD-Fkba(V91C) binding to the FRB domain is due to complete occupation of the AD-Fkba active site by another AD-Fkba molecule forming the dimer, as we expect this type of self-interaction to be transient. Similarly, because the cytoplasm and nucleus are reducing environments, we do not think the Fkba(V91C) disulfide-linked dimer will be a predominant species under these

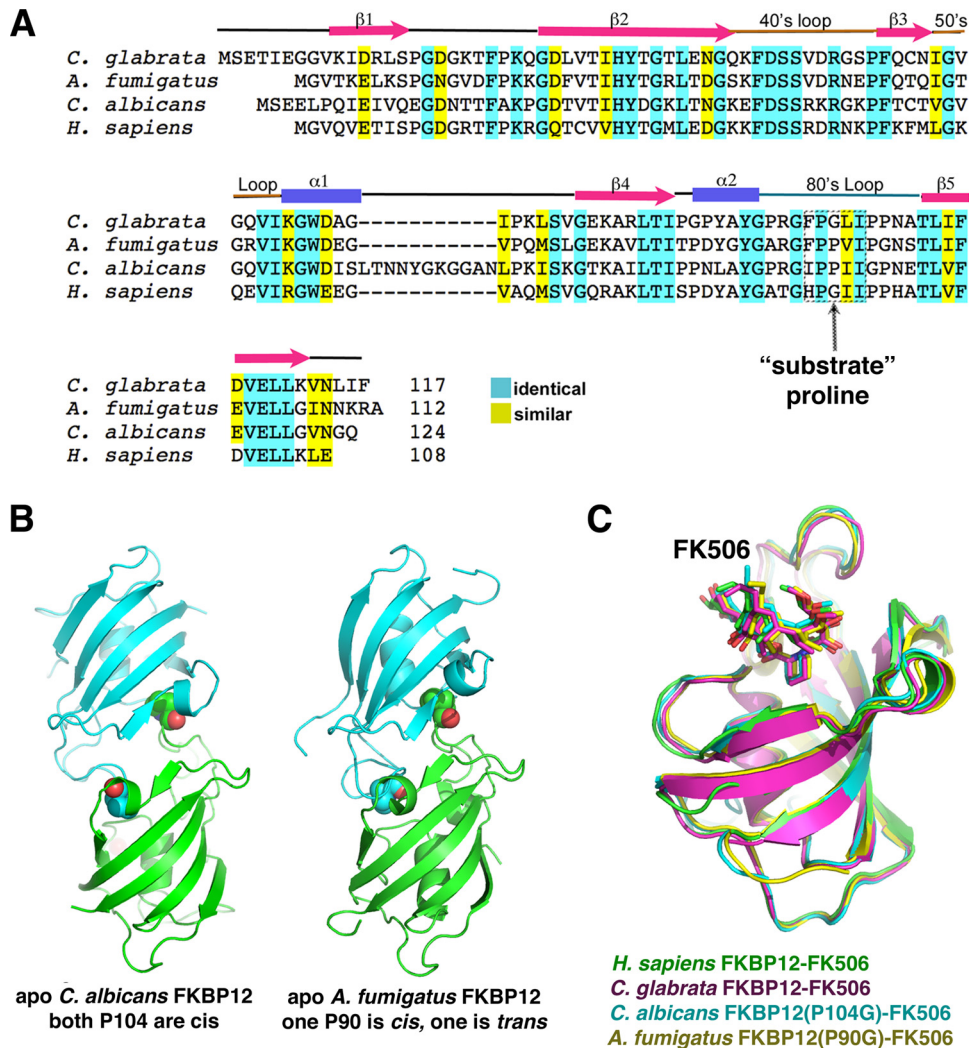


FIG 4 Alignment of FKBP12 sequences. The 80s loop proline is conserved in *C. albicans* and *A. fumigatus* FKBP12 but not in *C. glabrata*, and *H. sapiens* FKBP12s. (A) Sequence alignments of the FKBP12s of *C. albicans*, *A. fumigatus*, *C. glabrata*, and *H. sapiens*. Secondary structural elements are shown above the sequence. Identical and highly conserved residues are highlighted in cyan and yellow, respectively. (B) The *A. fumigatus* FKBP12 apo structure shows the same self-interaction as *C. albicans* FKBP12. Shown side by side are the self-interacting dimers of *A. fumigatus* and *C. albicans*. The proline corresponding to *C. albicans* Pro104 is Pro90 in *A. fumigatus* FKBP12, and interestingly, the *A. fumigatus* structure shows one subunit with Pro90 in the *cis* conformation and one with Pro90 in the *trans* conformation. (C) Superimpositions of the FKBP12-FK506 structures of *H. sapiens*, *C. albicans*, *C. glabrata*, and *A. fumigatus*, all showing the identical mode of FK506 binding.

conditions. It is possible that the conformation of the 80s loop in WT Fkba (or V91C) versus Fkba(P90G) influences the binding of the FKBP12-rapamycin complex to the FRB domain of the TOR protein.

***A. fumigatus* FKBP12(P90G) and FKBP12(V91C) mutations confer FK506 resistance.** On the basis of our structural and biochemical studies, the FKBP12(P90G) mutant would be predicted to be unable to self-catalyze, while the FKBP12(V91C) mutant might have altered target-binding properties. To test this, *A. fumigatus* strains expressing FKBP12(P90G) and FKBP12(V91C) tagged with enhanced green fluorescent protein (GFP) were generated and assessed for susceptibility to FK506 treatment (Fig. 6A to C). The stability of the respective mutated proteins was verified by Western analysis (Fig. 6C). As shown in Fig. 6A, both of the mutations induced relative FK506 resistance. FKBP12(V91C) exhibited greater resistance to FK506 than FKBP12(P90G) did

(Fig. 6A; see Fig. S4 in the supplemental material), indicating a potential loss of affinity for CaN. In order to examine the binding of the mutated FKBP12s to CaN, we also screened for their intracellular localization in the absence or presence of FK506. In the absence of FK506, FKBP12(P90G) and FKBP12(V91C) localized evenly throughout the cytoplasm and also in the nuclei (Fig. 6B). Upon exposure to FK506, septal localization in a disc-like pattern, as noted earlier with CaN, was evident (Fig. 6B). Interestingly, however, both the FKBP12(P90G) and FKBP12(V91C) proteins were still able to bind to CaN at the septa but to a lesser extent than WT FKBP12. Furthermore, FKBP12(V91C) showed 40 to 50% less septal localization than WT FKBP12, confirming its lower affinity for CaN. These observations support the idea that the sequence and conformation of the 80s loop can influence fungal FKBP12-FK506 binding to CaN, in accordance with previous studies of human FKBP12-FK506 binding to CaN (41).

TABLE 3 Data collection and refinement statistics for *C. glabrata* FKBP12 structures

Parameter	Apo <i>C. glabrata</i> FKBP12	<i>C. glabrata</i> FKBP12-FK506
Space group	I422	P6 ₃
Cell dimensions		
<i>a</i> , <i>b</i> , <i>c</i> (Å)	76.44, 76.44, 87.0	77.8, 77.8, 53.6
α , β , γ (°)	90.0, 90.0, 90.0	90.0, 90.0, 120.0
Resolution (Å)	43.5–2.65	42.0–1.30
<i>R</i> _{merge} (%)	12.0 (36.6) ^a	4.6 (41.4)
<i>I</i> / σ - <i>I</i>	11.8 (2.8)	11.7 (1.7)
Completeness (%)	98.7 (47.3)	97.7 (93.3)
Redundancy	3.3 (2.2)	3.6 (2.0)
Refinement		
Resolution (Å)	43.5–2.65	42.0–1.30
<i>R</i> _{work} / <i>R</i> _{free} (%)	21.4/26.0	15.3/16.4
No. of atoms		
Protein	873	873
Water	17	246
RMSD		
Bond length (Å)	0.003	0.025
Bond angle (°)	0.73	2.14

^a Values in parentheses are for the highest-resolution shell.

DISCUSSION

The FKBP12s of the pathogenic fungi *A. fumigatus*, *C. albicans*, and *C. glabrata* have emerged as potential targets for drug design because of their role in the inhibition of CaN, a critical component of a cell signaling pathway essential for fungal pathogenesis (31). FKBP12 inhibits CaN by binding the immunosuppressant FK506. This FKBP12-FK506 complex then docks onto CaN, preventing it from binding substrates. Hence, the design of fungus-specific inhibitors of this complex would be greatly aided by structures of fungal FKBP12s in the presence or absence of FK506 and FK506-like compounds. Therefore, we undertook the determination of the structures of the *A. fumigatus*, *C. albicans*, and *C. glabrata* FKBP12s in their apo and FK506-bound forms. The apo structures of the *A. fumigatus* and *C. albicans* proteins all revealed the unexpected finding that one of the loops, the 80s loop, is inserted into the active-site pocket of an adjacent subunit. This finding led to the hypothesis that the *A. fumigatus* and *C. albicans* FKBP12s may function to isomerize their own proline residues. Support for this notion comes from previous mutagenesis studies (36) that revealed that the central hydrophobic pocket where the prolines from the 80s loop bind is indeed the location of the PPIase active site. However, despite the large number of FKBP structures solved to date, no structure of an FKBP bound to a substrate is currently available, which has left the details of the PPIase mechanism unclear and has limited structure-based targeting design efforts. Thus, if the *A. fumigatus* and *C. albicans* FKBP12 apo structures have captured a self-substrate interaction, this would be significant, as it would indicate that these represent the first FKBP-substrate complex structures. Support for this hypothesis was provided by the analysis of a cysteine mutant form of the *A. fumigatus* protein that trapped the interacting dimer.

The possibility that the 80s loop of the fungal proteins might function as a self-substrate would be of interest from a physiological standpoint, as studies have highlighted the 80s loop as a key region in the interactions of FKBP12s with other proteins (26). As *cis/trans* isomerization impacts the conformation of this loop, it would therefore significantly impact the functions of FKBP12 outside their PPIase activity. Indeed, FKBP12s, which are ubiquitous

molecules with homologs found in bacteria to higher eukaryotes, carry out a wide range of functions, including roles outside their PPIase activity (26). For example, studies with mice revealed that FKBP12 is critical for modulating the calcium release activity of both skeletal and cardiac ryanodine receptors (42). FKBP12 was also shown to be a regulator of the cell cycle through its effect on transforming growth factor beta receptor signaling (20). However, the specific functions of FKBP12 appear to vary dramatically between organisms. This diversity of FKBP functions has made analyzing the contributions of PPIase activity versus effector protein binding difficult and also indicates that the role of FKBP12 in each organism must be dissected individually. In this regard, it is currently not possible to obtain a clear genetic assessment of the hypothesis that the *A. fumigatus* and *C. albicans* FKBP12s act as their own substrates because the cellular roles of these proteins in these fungi have yet to be elucidated. Therefore, further studies are needed to deduce the potential importance of *A. fumigatus* and *C. albicans* FKBP12 self-catalysis and its possible effects on isomerization targets and interacting proteins and their impacts on resultant cellular pathways.

MATERIALS AND METHODS

Protein expression and purification. Genes encoding the *C. albicans* and *A. fumigatus* FKBP12s that were codon optimized for *E. coli* expression were purchased from the GenScript Corporation (Piscataway, NJ) and subcloned into pET15b such that a hexahistidine tag (His tag), cleavable by thrombin, was added to the N termini. The proteins were expressed in *E. coli* BL21(DE3) cells. For protein expression, cells were grown to an optical density at 600 nm of ~0.6 at 37°C. At that time, the temperature was reduced to 15°C and isopropyl- β -D-thiogalactopyranoside was added to a final concentration of 1 mM. The cultures were allowed to grow for an additional 14 to 16 h, and the cells were pelleted and lysed in purification buffer (300 mM NaCl, 20 mM Tris-HCl [pH 7.5], 20 mM imidazole). The proteins were purified from the soluble fraction of the lysate via Ni-nitrilotriacetic acid (NTA) chromatography. Fractions containing FKBP12 were pooled and treated with thrombin at 4°C for 14 to 16 h to remove the N-terminal His tag. The digested sample was then applied to an Ni-NTA column, and the flowthrough was collected and loaded onto a Superdex 75 size exclusion column (GE Healthcare) equilibrated in elution buffer (150 mM NaCl, 20 mM Tris-HCl [pH 7.5]). The fractions containing pure protein were pooled and concentrated for biochemical studies and crystallization.

Crystallization and determination of the structures of *A. fumigatus* and *C. albicans* FKBP12 apo and FK506 complexes. *C. albicans* FKBP12 was crystallized in three different space groups, P1, P2₁2₁2, and C2, by hanging-drop vapor diffusion. The P1 crystal form was obtained by using a mixture of 25% polyethylene glycol (PEG) 3000, 0.1 M NaCl, and 0.1 M Tris-HCl (pH 8.0) as a crystallization reagent. The P2₁2₁2 form grew in a solution of 2 M ammonium sulfate and 0.1 M citrate (pH 5.5), and the C2 crystal form was crystallized in a mixture of 25% PEG 8000, 0.1 M sodium acetate (pH 4.5), and 0.2 M lithium sulfate. Each hanging drop contained a 1:1 ratio of ~10 mg/ml protein to crystallization reagent. The crystallization reagent supplemented with 25% glycerol was used as a cryosolvent. For cryopreservation, the crystals were dipped for several seconds in the cryosolvent prior to their placement in the liquid nitrogen stream. The *C. albicans* FKBP12(P104G)-FK506 complex crystallized in the P2₁ space group in a mixture of 2 M ammonium sulfate, 0.1 M *N*-cyclohexyl-3-aminopropanesulfonic acid (CAPS)-NaOH (pH 10.5), and 0.2 M lithium sulfate. One millimole of FK506 was added to the protein prior to crystallization. A solution of 4 M ammonium sulfate was used as a cryoprotectant. *A. fumigatus* FKBP12 at a concentration of 20 mg/ml was crystallized in the P2₁2₁2₁ space group in a mixture of 2 M ammonium sulfate, 0.1 M Tris-HCl (pH 7.0), and 0.2 M lithium sulfate. A 4 M ammonium sulfate solution was used as a cryoprotectant. *A. fumigatus* FKBP12(P90G)-FK506 crystals were obtained by mixing 20 mg/ml pro-

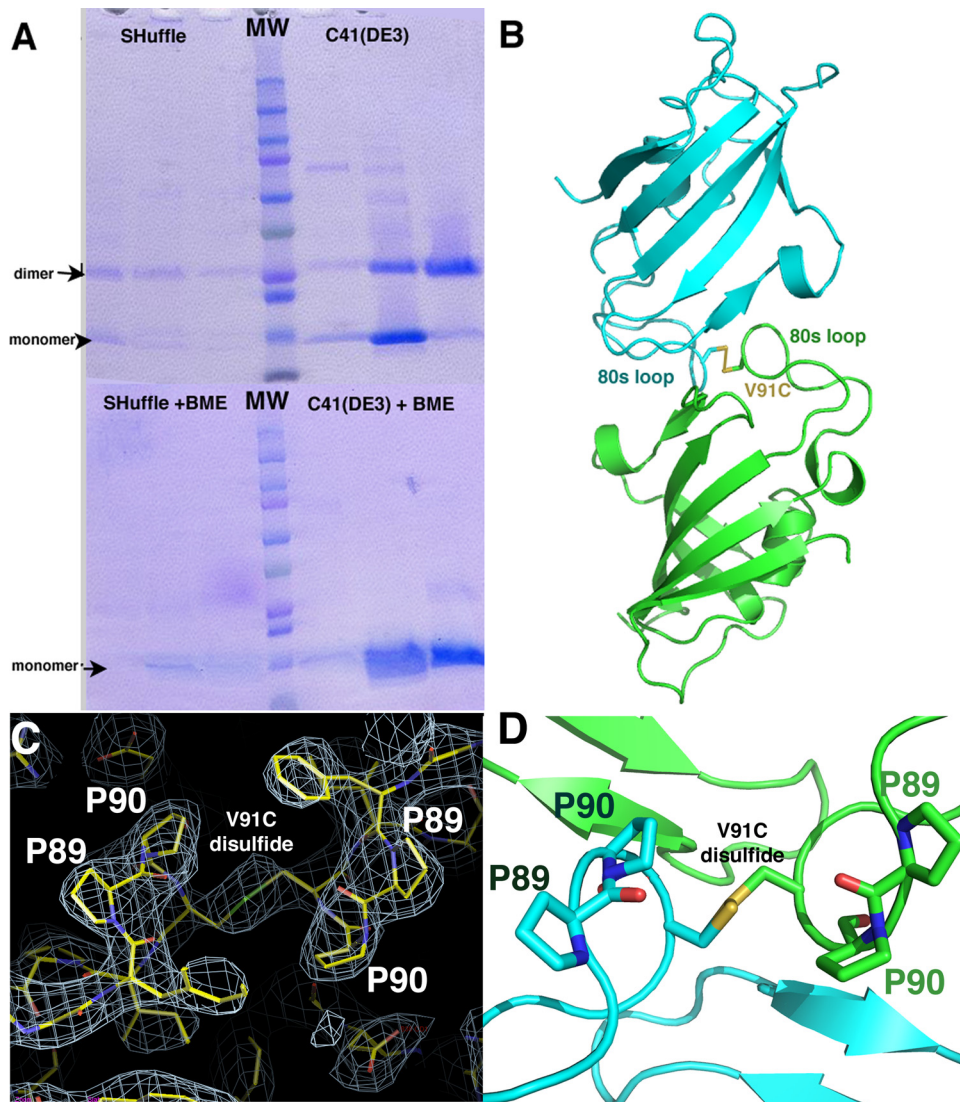


FIG 5 *A. fumigatus* FKBP12(V91C) mutation captures the intermolecular contact. (A) SDS-PAGE purification of FKBP12(V91C) from both SHuffle and C41(DE3) cells. Dimers are evident in the gel run without a reducing agent. Addition of a reducing agent leads to reduction of the disulfide bond and the proteins running as monomers. (B) Crystal structure of *A. fumigatus* FKBP12(V91C). (C) $2F_o - F_c$ electron density map contoured at 1σ showing the region around the V91C disulfide bond and the Pro89-Pro90 bond, which adopts a twisted, *trans* conformation-like state. (D) Ribbon diagram showing a closeup of the Pro89-Pro90 region with the residues labeled. Note that the green-labeled Pro90 side chains appear distorted.

tein (with 1 mM FK506) with a solution containing 2 M lithium sulfate, 0.1 M Tris-HCl (pH 8.5), and 2% PEG 400 at a 1:1 ratio. *C. albicans* FKBP12(P104G) apo crystals were grown by mixing protein at 10 mg/ml 1:1 with a combination of 2 M ammonium sulfate, 0.1 M CAPS (pH 10.5), and 0.2 M lithium sulfate. The crystals could be cryopreserved straight from the drop. Data were collected at Advanced Light Source beamline 8.3.1 or Advanced Photon Source. Data were processed with HKL3000 or MOSFLM. Initial phases were obtained in each case by using molecular replacement (MolRep), starting with the human FKBP12 model (PDB code 2PPN). The *A. fumigatus* and *C. glabrata* apo structures were solved by using the *C. albicans* apo high-resolution structure as a starting model in MolRep. The FK506-bound structures were solved by using the requisite apo structures as starting models. All model building was carried out with COOT or O, and refinements were performed in PHENIX (42).

Mutant *A. fumigatus* FKBP12(V91C) construction, disulfide cross-linking experiments, and determination of the structure of the cross-linked dimer. Mutant *A. fumigatus* FKBP12(V91C) was made with the

QuikChange kit. The pET15b plasmid expressing the mutant protein was transformed into C41 (DE3) and SHuffle cells. The protein was expressed and purified in the same way as WT *A. fumigatus* FKBP12, except that no reducing agent was added at any step. The *A. fumigatus* FKBP12(V91C) dimer was separated from the monomer via size exclusion chromatography, and the His tag was cleaved before crystallization trials. The protein was concentrated to 30 mg/ml, and crystals were grown by mixing the protein solution 1:1 with a reservoir consisting of 1.5 M sodium citrate and 0.1 M sodium cacodylate (pH 6.5). Crystals grew within 3 h and were cryopreserved by being dipped for 1 s in a drop containing the crystallization solution supplemented with 25% glycerol. Data were collected and processed with MOSFLM. The structure was solved by MolRep with the *A. fumigatus* apo structure as a search model. The structure was refined with PHENIX (43).

Construction of *A. fumigatus* FKBP12(P90G) and FKBP12(V91C) strains. *A. fumigatus* WT strain *akuB^{KU80}* was used for all transformation experiments and grown on glucose minimal medium (GMM) at 37°C

TABLE 4 Interactions of FKBP12, FKBP12 variants, and the FRB domain determined by Y2H analysis

AD-gene fusion	BD-gene fusion	Interaction	Drug ^b
N termini^a			
FKBP12	FRB	—	Rapamycin
FKBP12	FRB	—	
FKBP12(P90G)	FRB	+	Rapamycin
FKBP12(P90G)	FRB	—	
FKBP12(V91C)	FRB	—	Rapamycin
FKBP12(V91C)	FRB	—	
FRB	FKBP12	+	Rapamycin
FRB	FKBP12	—	
FRB	FKBP12(P90G)	+	Rapamycin
FRB	FKBP12(P90G)	—	
FRB	FKBP12(V91C)	+	Rapamycin
FRB	FKBP12(V91C)	—	
C termini^c			
FKBP12	FRB	+	Rapamycin
FKBP12	FRB	—	
FKBP12(P90G)	FRB	+	Rapamycin
FKBP12(P90G)	FRB	—	
FKBP12(V91C)	FRB	+	Rapamycin
FKBP12(V91C)	FRB	—	
FKBP12	FKBP12	—	Rapamycin
FKBP12	FKBP12	—	FK506
FKBP12	FKBP12	—	
FKBP12(P90G)	FKBP12(P90G)	—	Rapamycin
FKBP12(P90G)	FKBP12(P90G)	—	FK506
FKBP12(P90G)	FKBP12(P90G)	—	
FKBP12(P90G)	FKBP12(P90G)	—	
FKBP12(V91C)	FKBP12(V91C)	—	Rapamycin
FKBP12(V91C)	FKBP12(V91C)	—	FK506
FKBP12(V91C)	FKBP12(V91C)	—	

^a N termini of FKBP12s were fused with the GAL4 AD.^b Both rapamycin and FK506 were used at 1 μ g/ml.^c C termini of FKBP12s were fused with the GAL4 AD.

(44). In certain experiments, GMM agar or RPMI liquid medium was supplemented with FK506 (0.1 to 10 μ g/ml). All radial-growth experiments were repeated three times, each in triplicate. *E. coli* DH5 α competent cells were used for subcloning. Site-directed mutagenesis of two FKBP12 residues (P90G and V91C) was performed with the primers listed in Table S2 in the supplemental material and the pUCGH-FKBP12 plasmid (45), consisting of 384 bp of the 637-bp *fkbp12* gene (*fkbp12*/Afu6g12170, <http://www.aspergillusgenome.org>) and ~1 kb of the *fkbp12* terminator sequence as the template. Briefly, in the first PCR, two fragments were amplified with complementary primers (with respective mutations) overlapping the *fkbp12* region to be mutated and the respective primers at the N and C termini of *fkbp12*. No stop codon was introduced at the C-terminal end of *fkbp12* to facilitate expression of the *gfp* fusion. Next, fusion PCR was done with equiproportional mixtures of the two PCR fragments as the templates, and the final mutated 384-bp *fkbp12* PCR fragment was amplified with primers at the N and C termini of *fkbp12* (see Table S2 in the supplemental material). Mutated *fkbp12* fragments were digested with KpnI and BamHI and cloned into the pUCGH-FKBP12 plasmid by replacing the 384-bp WT *fkbp12* PCR fragment to facilitate homologous integration. Mutated *fkbp12* genes were sequenced (see Table S2 for the primers used) to confirm the mutation and linearized with KpnI for homologous integration. Linearized constructs were transformed into *A. fumigatus* *akuB*^{KU80}, and transformants were selected with hygromycin B (150 μ g/ml) as previously described (46). Transformants were verified for homologous integration by PCR (see Table S2 and Fig. S5 in the supplemental material) and verified for accuracy of mutation by sequencing and fluorescence microscopy.

Protein extraction and Western analysis. *A. fumigatus* recombinant strains expressing respective WT and mutated forms of FKBP12-GFP fusion proteins were cultured in liquid GMM at 200 rpm for 24 h at 37°C. Crude extracts were prepared as previously described (47). Approximately 50 μ g of protein electrophoresed on a 4 to 20% SDS-polyacrylamide gel was transferred onto a polyvinylidene difluoride

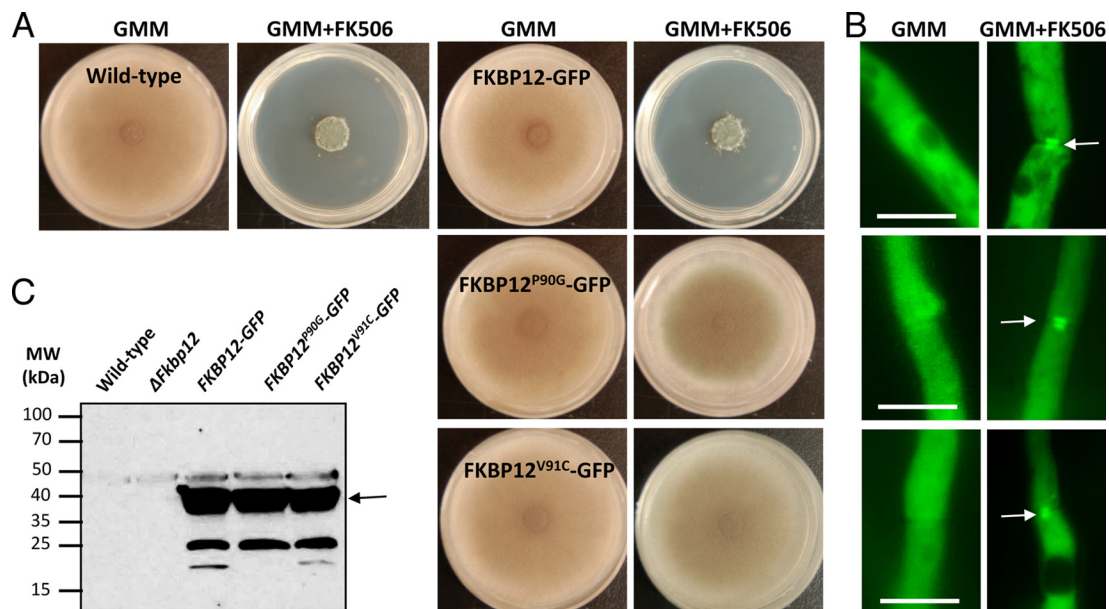


FIG 6 *In vivo* analysis of mutant *A. fumigatus* FKBP12s. (A) Radial growth of the WT strain (*akuB*^{KU80}) and the strains expressing WT FKBP12-GFP and the mutated versions of FKBP12 [FKBP12(P90G) and FKBP12(V91C)] tagged with GFP were assessed after 5 days on GMM agar with or without supplementation with FK506 (100 ng/ml). Note the resistance of the FKBP12(P90G)- and FKBP12(V91C)-producing strains to FK506. (B) Strains expressing WT FKBP12-GFP and the mutated versions of FKBP12 [FKBP12(P90G) and FKBP12(V91C)] tagged with GFP were cultured in liquid GMM in the absence or presence of FK506 (100 ng/ml) on coverslips for 18 to 20 h and observed for the localization of FKBP12 by fluorescence microscopy. Note the complete cytosolic localization of FKBP12s in the absence of FK506. Arrows indicate the translocation of FKBP12s to the hyphal septa in the presence of FK506 indicative of their binding to CaN at the hyphal septa. Scale bar, 10 μ m. (C) Western analysis performed with the anti-GFP polyclonal primary antibody and a peroxidase-labeled anti-rabbit IgG secondary antibody. The arrow indicates the ~37-kDa FKBP12-GFP fusion protein. The values on the left are molecular masses in kilodaltons.

membrane (Bio-Rad) and probed with a rabbit polyclonal antibody. The anti-GFP primary antibody (1 $\mu\text{g}/\text{ml}$; GenScript) and peroxidase-labeled rabbit anti-IgG (1:5,000; Rockland) secondary antibody. Detection was performed with SuperSignal West Pico Chemiluminescent Substrate (Thermo Scientific).

Microscopy. Conidia (10^4) from the recombinant strains of *A. fumigatus* were inoculated into 5 ml of GMM, poured over a sterile coverslip (22 by 60 mm; no. 1), and placed in a sterile dish (60 by 15 mm). Cultures grown for 18 to 20 h at 37°C were observed by fluorescence microscopy with an Axioskop 2 plus microscope (Zeiss) equipped with AxioVision 4.6 imaging software.

Y2H analysis. The *A. fumigatus* *fkbA* gene and its variants, including *fkbA*^{P90G} and *fkbA*^{V91C} and the FRB domain-encoding gene were synthesized after codon optimization for *S. cerevisiae* expression (GenScript) and cloned into pGADT7 or pGBKT7 (Clontech Laboratories Inc.) for Y2H analysis. *S. cerevisiae* SMY4-1, which lacks the FKBP12 gene (*FPR1*), was used to examine the interactions. β -Galactosidase assays were performed as previously described (38, 39).

SUPPLEMENTAL MATERIAL

Supplemental material for this article may be found at <http://mbio.asm.org/lookup/suppl/doi:10.1128/mBio.00492-16/-/DCSupplemental>.

Figure S1, TIF file, 0.3 MB.

Figure S2, TIF file, 0.5 MB.

Figure S3, TIF file, 0.2 MB.

Figure S4, TIF file, 0.8 MB.

Figure S5, TIF file, 0.3 MB.

Table S1, DOC file, 0.1 MB.

Table S2, DOC file, 0.03 MB.

ACKNOWLEDGMENTS

Beamline 8.3.1 at the Advanced Light Source is operated by the University of California Office of the President, Multicampus Research Programs and Initiatives grant MR-15-328599 and the Program for Breakthrough Biomedical Research, which is partially funded by the Sandler Foundation. This research used resources of the Advanced Photon Source, a U.S. Department of Energy (DOE) Office of Science User Facility operated for the DOE Office of Science by the Argonne National Laboratory under contract DE-AC02-06CH11357. This work was supported by NIH/NIAID multi-PI R01 award AI112595 and P01 award AO104533 to J.H., L.S., W.S., and M.A.S. J.H. also received support from NIH/NIAID R43 SBIR grant R43 AI098300-01 and an Astellas Pharma Global Development Research grant.

FUNDING INFORMATION

This work was funded by HHS | NIH | National Institute of Allergy and Infectious Diseases (NIAID) (AI112595). This work was funded by HHS | NIH | National Institute of Allergy and Infectious Diseases (NIAID) (AI104533).

REFERENCES

- Brandts JF, Halvorson HR, Brennan M. 1975. Consideration of the possibility that the slow step in protein denaturation reactions is due to cis-trans isomerism of proline residues. *Biochemistry* 14:4953–4963. <http://dx.doi.org/10.1021/bi00693a026>.
- Schmid FX, Baldwin RL. 1978. Acid catalysis of the formation of the slow-folding species of RNase A: evidence that the reaction is proline isomerization. *Proc Natl Acad Sci U S A* 75:4764–4768. <http://dx.doi.org/10.1073/pnas.75.10.4764>.
- Schmid FX, Buchner J, Kiefhaber T. 2005. Prolyl isomerization in protein folding, p 916–945. In Buchner J, Kiefhaber T (ed), *Protein folding handbook*. Wiley-VCH, Weinheim, Germany.
- Schmid FX, Lang K, Kiefhaber T, Mayer S, Schönbrunner R. 1991. Prolyl isomerase: its role in protein folding and speculations on its function in the cell. In Nall BT, Dill KA (ed), *Conformations and forces in protein folding*. American Association for the Advancement of Science, Washington, DC.
- Yaffe MB, Schutkowski M, Shen M, Zhou XZ, Stukenberg PT, Rahfeld JU, Xu J, Kuang J, Kirschner MW, Fischer G, Cantley LC, Lu KP. 1997. Sequence-specific and phosphorylation-dependent proline isomerization—a potential mitotic regulatory mechanism. *Science* 278:1957–1960. <http://dx.doi.org/10.1126/science.278.5345.1957>.
- Mallis RJ, Brazin KN, Fulton DB, Andreotti AH. 2002. Structural characterization of a proline-driven conformational switch within the Itk SH2 domain. *Nat Struct Biol* 9:900–905. <http://dx.doi.org/10.1038/nsb864>.
- Andreotti AH. 2003. Native state proline isomerization: an intrinsic molecular switch. *Biochemistry* 42:9515–9524. <http://dx.doi.org/10.1021/bi0350710>.
- Fischer G, Aumüller T. 2003. Regulation of peptide bond cis/trans isomerization by enzyme catalysis and its implication in physiological processes. *Rev Physiol Biochem Pharmacol* 148:105–150. <http://dx.doi.org/10.1007/s10254-003-0011-3>.
- Eckert B, Martin A, Balbach J, Schmid FX. 2005. Prolyl isomerization as a molecular timer in phage infection. *Nat Struct Mol Biol* 12:619–623. <http://dx.doi.org/10.1038/nsmb946>.
- Fanghänel J, Fischer G. 2004. Insights into the catalytic mechanism of peptidyl prolyl cis/trans isomerases. *Front Biosci* 9:3453–3478. <http://dx.doi.org/10.2741/1494>.
- Eckert B, Schmid FX. 2007. A conformational unfolding reaction activates phage fd for the infection of *Escherichia coli*. *J Mol Biol* 373:452–461. <http://dx.doi.org/10.1016/j.jmb.2007.07.060>.
- Sarkar P, Reichman C, Saleh T, Birge RB, Kalodimos CG. 2007. Proline cis-trans isomerization controls autoinhibition of a signaling protein. *Mol Cell* 25:413–426. <http://dx.doi.org/10.1016/j.molcel.2007.01.004>.
- Lu KP, Finn G, Lee TH, Nicholson LK. 2007. Prolyl cis-trans isomerization as a molecular timer. *Nat Chem Biol* 3:619–629. <http://dx.doi.org/10.1038/nchembio.2007.35>.
- Ke HM, Zydowsky LD, Liu J, Walsh CT. 1991. Crystal structure of recombinant human T-cell cyclophilin A at 2.5-Å resolution. *Proc Natl Acad Sci U S A* 88:9483–9487. <http://dx.doi.org/10.1073/pnas.88.21.9483>.
- Mikol V, Kallen J, Pflügl G, Walkinshaw MD. 1993. X-ray structure of a monomeric cyclophilin A-cyclosporin A crystal complex at 2.1-Å resolution. *J Mol Biol* 234:1119–1130. <http://dx.doi.org/10.1006/jmbi.1993.1664>.
- Ranganathan R, Lu KP, Hunter T, Noel JP. 1997. Structural and functional analysis of the mitotic rotamase Pin1 suggests substrate recognition is phosphorylation dependent. *Cell* 89:875–886. [http://dx.doi.org/10.1016/S0092-8674\(00\)80273-1](http://dx.doi.org/10.1016/S0092-8674(00)80273-1).
- Leulliot N, Vicentini G, Jordens J, Quevillon-Cheruel S, Schiltz M, Barford D, van Tilbeurgh H, Goris J. 2006. Crystal structure of the PP2A phosphatase activator: implications for its PP2A-specific PPIase activity. *Mol Cell* 23:413–424. <http://dx.doi.org/10.1016/j.molcel.2006.07.008>.
- Michnick SW, Rosen MK, Wandless TJ, Karplus M, Schreiber SL. 1991. Solution structure of FKBP, a rotamase enzyme and receptor for FK506 and rapamycin. *Science* 252:836–839. <http://dx.doi.org/10.1126/science.1709301>.
- Van Duynne GD, Standaert RF, Karplus PA, Schreiber SL, Clardy J. 1991. Atomic structure of FKBP-FK506, an immunophilin-immunosuppressant complex. *Science* 252:839–842. <http://dx.doi.org/10.1126/science.1709302>.
- Aghdasi B, Ye K, Resnick A, Huang A, Ha HC, Guo X, Dawson TM, Dawson VL, Snyder SH. 2001. FKBP12, the 12-kDa FK506-binding protein, is a physiologic regulator of the cell cycle. *Proc Natl Acad Sci U S A* 98:2425–2430. <http://dx.doi.org/10.1073/pnas.041614198>.
- Harrison RK, Stein RL. 1990. Substrate specificities of the peptidyl prolyl cis-trans isomerase activities of cyclophilin and FK-506 binding protein: evidence for the existence of a family of distinct enzymes. *Biochemistry* 29:3813–3816. <http://dx.doi.org/10.1021/bi00468a001>.
- Stein RL. 1993. Mechanism of enzymatic and nonenzymatic prolyl cis-trans isomerization. *Adv Protein Chem* 44:1–24. [http://dx.doi.org/10.1016/S0065-3233\(08\)60562-8](http://dx.doi.org/10.1016/S0065-3233(08)60562-8).
- Park ST, Aldape RA, Futer O, DeCenzo MT, Livingston DJ. 1992. PPIase catalysis by human FK506-binding protein proceeds through a conformational twist mechanism. *J Biol Chem* 267:3316–3324.
- Schreiber SL. 1991. Chemistry and biology of the immunophilins and their immunosuppressive ligands. *Science* 251:283–287. <http://dx.doi.org/10.1126/science.1702904>.
- Sigal NH, Dumont FJ. 1992. Cyclosporin A, FK-506 and rapamycin: pharmacologic probes of lymphocyte signal transduction. *Annu Rev Immunol* 10:519–560. <http://dx.doi.org/10.1146/annurev.iy.10.040192.002511>.

26. Schreiber SL, Crabtree GR. 1995. Immunophilins, ligands and the control of signal transduction. *Harvey Lect* 91:99–114.
27. Kang CB, Hong Y, Dhe-Paganon S, Yoon HS. 2008. FKBP family proteins: immunophilins with versatile biological functions. *Neurosignals* 16:318–325. <http://dx.doi.org/10.1159/000123041>.
28. Hemenway CS, Heitman J. 1999. Calcineurin. Structure, function and inhibition. *Cell Biochem Biophys* 30:115–151. <http://dx.doi.org/10.1007/BF02737887>.
29. Im SH, Rao A. 2004. Activation and deactivation of gene expression by Ca²⁺/calcineurin-NFAT-mediated signaling. *Mol Cells* 18:1–9.
30. Clipstone NA, Crabtree GR. 1992. Identification of calcineurin as a key signaling enzyme in T-lymphocyte activation. *Nature* 357:695–697. <http://dx.doi.org/10.1038/357695a0>.
31. Steinbach WJ, Reedy JL, Cramer RA, Jr, Perfect JR, Heitman J. 2007. Harnessing calcineurin as a novel anti-infective agent against invasive fungal infections. *Nat Rev Microbiol* 5:418–430. <http://dx.doi.org/10.1038/nrmicro1680>.
32. O'Keefe SJ, Tamura J, Kincaid RL, Tocci MJ, O'Neill EA. 1992. FK-506 and CsA-sensitive activation of the interleukin-2 promoter by calcineurin. *Nature* 357:692–694. <http://dx.doi.org/10.1038/357692a0>.
33. Galat A. 2013. Functional diversity and pharmacological profiles of the FKBP5s and their complexes with small natural ligands. *Cell Mol Life Sci* 70:3243–3275. <http://dx.doi.org/10.1007/s00018-012-1206-z>.
34. Dornan J, Taylor P, Walkinshaw MD. 2003. Structures of immunophilins and their ligand complexes. *Curr Top Med Chem* 3:1392–1409. <http://dx.doi.org/10.2174/1568026033451899>.
35. Alag R, Balakrishna AM, Rajan S, Qureshi IA, Shin J, Lescar J, Grüber G, Yoon HS. 2013. Structural insights into substrate binding by PvFKBP35, a peptidylprolyl *cis-trans* isomerase from the human malarial parasite *Plasmodium vivax*. *Eukaryot Cell* 12:627–634. <http://dx.doi.org/10.1128/EC.00016-13>.
36. Ikura T, Ito N. 2007. Requirements for peptidyl-prolyl isomerization activity: a comprehensive mutational analysis of the substrate-binding cavity of FK506-binding protein 12. *Protein Sci* 16:2618–2625. <http://dx.doi.org/10.1110/ps.073203707>.
37. Ikura T, Kinoshita K, Ito N. 2008. A cavity with an appropriate size is the basis of the PPIase activity. *Protein Eng Des Sel* 21:83–89. <http://dx.doi.org/10.1093/protein/gzm087>.
38. Cardenas ME, Hemenway C, Muir RS, Ye R, Fiorentino D, Heitman J. 1994. Immunophilins interact with calcineurin in the absence of endogenous immunosuppressive ligands. *EMBO J* 13:5944–5957.
39. Bastidas RJ, Shertz CA, Lee SC, Heitman J, Cardenas ME. 2012. Rapamycin exerts antifungal activity *in vitro* and *in vivo* against *Mucor circinelloides* via FKBP12-dependent inhibition of Tor. *Eukaryot Cell* 11:270–281. <http://dx.doi.org/10.1128/EC.05284-11>.
40. Cruz MC, Blankenship J, Del Poeta M, Perfect JR, McCusker JH, Bennai YL, Cardenas ME, Heitman J. 2001. Rapamycin and less immunosuppressive analogs are toxic to *Candida albicans* and *Cryptococcus neoformans* via FKBP12-dependent inhibition of TOR. *Antimicrob Agents Chemother* 45:3162–3170. <http://dx.doi.org/10.1128/AAC.45.11.3162-3170.2001>.
41. Futer O, DeCenzo MT, Aldape RA, Livingston DJ. 1995. FK506 binding protein mutational analysis. Defining the surface residue contributions to stability of the calcineurin co-complex. *J Biol Chem* 270:18935–18940. <http://dx.doi.org/10.1074/jbc.270.32.18935>.
42. Shou W, Aghdasi B, Armstrong DL, Guo Q, Bao S, Charng MJ, Mathews LM, Schneider MD, Hamilton SL, Matzuk MM. 1998. Cardiac defects and altered ryanodine receptor function in mice lacking FKBP12. *Nature* 391:489–492. <http://dx.doi.org/10.1038/35146>.
43. Adams PD, Afonine PV, Bunkóczi G, Chen VB, Echols N, Headd JJ, Hung LW, Jain S, Kapral GJ, Grosse-Kunstleve RW, McCoy AJ, Moriarty NW, Oeffner R, Read RJ, Richardson DC, Richardson JS, Terwilliger TC, Zwart PH. 2010. PHENIX: a comprehensive Python-based system for macromolecular structure solution. *Acta Crystallogr D* 66:213–221. <http://dx.doi.org/10.1107/S0907444909052925>.
44. Shimizu K, Keller NP. 2001. Genetic involvement of a cAMP-dependent protein kinase in a G protein signaling pathway regulating morphological and chemical transitions in *Aspergillus nidulans*. *Genetics* 157:591–600.
45. Falloon K, Juvvadi PR, Richards AD, Vargas-Muniz JV, Renshaw H, Steinbach WJ. 2015. Characterization of the Fkbp12-encoding genes in *Aspergillus fumigatus*. *PLoS One* 10:e0137869. <http://dx.doi.org/10.1371/journal.pone.0137869>.
46. Steinbach WJ, Cramer RA, Jr., Perfect BZ, Asfaw YG, Sauer TC, Najvar LK, Kirkpatrick WR, Patterson TF, Benjamin DK, Jr., Heitman J, Perfect JR. 2006. Calcineurin controls growth, morphology, and pathogenicity in *Aspergillus fumigatus*. *Eukaryot Cell* 5:1091–1103. <http://dx.doi.org/10.1128/EC.00139-06>.
47. Juvvadi PR, Fortwendel JR, Rogg LE, Burns KA, Randell SH, Steinbach WJ. 2011. Localization and activity of the calcineurin catalytic and regulatory subunit complex at the septum is essential for hyphal elongation and proper septation in *Aspergillus fumigatus*. *Mol Microbiol* 82:1235–1259. <http://dx.doi.org/10.1111/j.1365-2958.2011.07886.x>.